

# **EXECUTIVE SUMMARY**

# Demonstration of Artificial Intelligence Leak Detection Technology for Real-Time Drinking Water Distribution System Leak Monitoring

Hunter Klein
Andrew Drucker
Steven Fann
Hunter Klein
Naval Facilities Command
Engineering and Expeditionary
Warfare Center

March 2024

# ESTCP EXECUTIVE SUMMARY

EW21-5093

## **TABLE OF CONTENTS**

	Page
INTRODUCTION	1
OBJECTIVES	2
TECHNOLOGY DESCRIPTION	2
3.1 TEST DESIGN	3
3.2 DEMONSTRATION TESTS	5
PERFORMANCE ASSESSMENT	7
4.2 LEAK DETECTION	9
4.4 LEAK LOCALIZATION	11
COST ASSESSMENT	12
IMPLEMENTATION ISSUES	13
REFERENCES	14
	3.2 DEMONSTRATION TESTS

# LIST OF FIGURES

-	Page
Figure ES-1.	Hydrant.AI for Wet Barrel Hydrants
Figure ES-2.	Demonstration Site Map
Figure ES-3.	Wet Barrel Hydrant, as Retrofitted with hydrant.AI
riguie ES 3.	Sensor Station at NBVC Port Hueneme Demonstration Site
Figure ES-4.	High-level System Architecture (Phase-II)
Figure ES-5.	A Leak Simulated at the Sampling Station During Phase-I Testing
Figure ES-6.	An Apparatus Attached to a Hydrant for Automating the Leak Flow
Figure ES-7.	hydrant.AI Sensor Backhaul with a Wireless Communication
υ	Module for Phase-II. 6
Figure ES-8.	Acoustic Summary for Flow Test with Details Shown in Table ES-1 8
Figure ES-9.	
C	Acoustic Data from a Flow Test (ref. Table ES-1), after
	Transformation of Data Into Leak Features
Figure ES-10	Overview of Baseline Learning & Leak Detection Model Testing Procedure 8
Figure ES-11	
	(a) Baseline (b) Leak Detection
Figure ES-12	· · · · · · · · · · · · · · · · · · ·
	System at Hydrant 3
Figure ES-13	Leak Location Estimate Obtained for an Optimal Cross-correlation
	Threshold from a Leak Simulated
	LIST OF TABLES
	Page
	8
Table ES-1.	Details of a Flow Test Conducted at the Location: Sampling Station
	Phase-I   19 Jan 20236
Table ES-2.	Details of Automated Flow Tests Conducted Overnight
	Over Multiple Days   Phase-I
Table ES-3.	Details of an Automated Flow Test Conducted at the Location
	Hydrant 2   Phase-II   1 Nov 2023–1 Mar 2024
Table ES-4.	Minimum Accuracy Returned by AI leak detection models
T 11 FC 5	on test datasets.
Table ES-5.	Life-cycle Cost Analysis

### **ACRONYMS AND ABBREVIATIONS**

AI artificial intelligence ATO authority to operate

DoD Department of Defense DWS Digital Water Solutions

ESTCP Environmental Security Technology Certification Program

EXWC Expeditionary Warfare Center

GPM gallons per minute

GPS global positioning system

iNFADS internet Navy Facilities Asset Data Store

NAVFAC Naval Facilities Engineering Systems Command

NBVC Naval Base Ventura County

PVC polyvinyl chloride

RMF risk management framework

ROI return on investment

UCLA University of California, Los Angeles

WDN water distribution network

### **ACKNOWLEDGMENTS**

The project team wishes to thank the Environmental Security Technology Certification Program (ESTCP) for funding and sponsoring this certification project. The project team is also grateful to the Office of Naval Research's Next Strategic Technology Evaluation Program for funding an initial evaluation study of the technology prior to pursuing its demonstration. The authors offer their gratitude to the installation Naval Base Ventura County (NBVC), Port Hueneme, California and their public works department personnel who provided the test and demonstration host facilities and the needed assistance and support throughout the certification effort. The project team also wants to acknowledge the Veterans To Energy Careers internship program for supporting Mr. Brian Vu, who greatly contributed to the success of the project.

### 1.0 INTRODUCTION

This report is the technical final report for the project titled "Demonstration of Artificial Intelligence (AI) Leak Detection Technology for Real-Time Drinking Water Distribution System Leak Monitoring". The demonstration addressed the need to identify leaks (identification covers both detection and localization) cost-effectively in Department of Defense (DoD) water distribution systems (2021 ESTCP Need # D8 Enhanced Installation Water Resiliency) through an online artificial intelligence (AI) leak detection system. The demonstration was conducted by Naval Facilities Engineering and Expeditionary Warfare Center (NAVFAC EXWC) at Naval Base Ventura County (NBVC) in Port Hueneme, California.

Recent studies [1], [2] showed that North America's water infrastructure is in a steep decline, manifesting in the form of increasingly prevalent water mains breaks and non-surfacing leaks. Beyond water loss, these types of events could also lead to flooding, service disruptions and increased strain on the distribution network. Pipe break rates have increased by an alarming 27% in the past six years. Data from the internet Navy Facilities Asset Data Store (iNFADS) showed that the majority of the Navy's water lines were either approaching or have exceeded their expected useful life, with 67% of water lines over 40 years old, and 37% over the age of 65. iNFADS also showed that 57% of the water line inventory was currently in either poor or failing condition, leading to an increasing likelihood of sudden water main breaks and non-surfacing leaks. In particular, non-surfacing leaks were challenging to address, as many of these leaks often remained undetected underground, resulting in significant water losses over time. Efficient strategies to detect and locate leaks in DoD's water distribution systems are needed to help improve water conservation efforts and enhance installation water system resiliency.

The leak detection technology deployed in the demonstration utilized a bespoke continuous monitoring technology (hydrant.AI) developed by Digital Water Solutions (DWS) in tandem with state-of-the-art leak localization algorithms developed by UCLA researchers. The hardware consisted of a set of sensing devices, retrofittable to any existing fire hydrant, that provided the ability to non-invasively detect and monitor for leaks and pressure transients within the water distribution network (WDN). Sensor data from the devices could be sent to a server asynchronously (i.e., offline) or in real-time (i.e., cellular based) where insights pertaining to leaks and pressure events were extracted using machine learning before being sent to a user interface and alert system. Unlike other monitoring technologies, which relied on listening for leaks through vibrations propagated through the pipe wall, the demonstrated technology used a hydrophone to listen for leaks directly in the water column. Crucially, this feature enabled the hydrant.AI system to detect leaks in polyvinyl chloride (PVC) networks where traditional vibration-based technologies struggled. Additionally, the hardware system was modified by DWS with bespoke firmware for this project to offer the ability to customize the various sampling parameters to meet the specific research and testing needs throughout each phase of the demonstration. The demonstration was conducted in two discrete phases. The first phase considered an offline, asynchronous implementation of the technology, where sensor data from each device was manually collected and uploaded to the server for processing, while the second phase demonstrated a fully online implementation in which sensor data could be automatically transmitted to the secured server in real-time via cellular connectivity.

### 2.0 OBJECTIVES

The main objective of the project was to demonstrate a new and powerful AI leak detection technology (detection technology is used synonymously with identification to include both leak detection and localization) for online leak monitoring in water distribution systems at DoD installations. The demonstration was intended to test and evaluate the performance of this technology by assessing its ability to detect and monitor leaks in a continuous monitoring setting. During the set-up phase and periodically afterward, labeled acoustic data was used to train the machine learning algorithms to differentiate leak-induced noise from confounding ambient noise sources. Following the initial training period, the system switched to a continuous monitoring mode to detect new leaks as they occurred in the network. The performance was assessed based on the capability to detect and localize known, simulated leak events. The system was also capable of detecting the occurrence of pressure transients (water hammers) and low/high-pressure events. The project also performed a life-cycle cost analysis to compare the costs against the expected water savings benefits generated by the technology over a 10-year period. Ultimately, the goal of the demonstration was to help validate and de-risk the adoption of novel leak detection technologies within DoD installations through provision of detailed information pertaining to the implementation, application, cost, and efficacy.

### 3.0 TECHNOLOGY DESCRIPTION

The demonstrated technology offered a unique and comprehensive solution for monitoring of WDNs. Unlike traditional surface-mounted vibration sensors, which are ineffective in detecting and locating leaks in plastic (i.e., PVC) pipes, the demonstrated technology utilized a hydrophone inserted directly in the water column to listen for leaks. This approach made the technology effective at capturing leak noise regardless of the pipe material, while also providing the ability to capture leaks over longer distances relative to traditional vibration sensors. In tandem with the state-of-the-art hardware, the technology used novel AI and probabilistic methods to identify and locate leaks in the collected acoustic data. The AI algorithms for leak detection—developed by DWS—eliminated the need for historical data or pre-existing information regarding the network layout or pipe material, which drastically simplified the onboarding process. The leak localization algorithm used in the demonstration was developed at UCLA based on maximum likelihood estimation—a powerful localization technique that is widely used in wireless networks.

With respect to hardware, the original design was intended for deployment in dry-barrel fire hydrants. To accommodate the type of hydrant typical to NBVC and California (i.e., wet-barrel), a new wet-barrel configuration for hydrant.AI was designed, prototyped, fabricated, and tested by DWS prior to deployment at NBVC. The hardware component primarily consisted of a hydrant retrofit kit (shown in Figure ES-1) that included a sensing array (hydrophone, thermocouple, and pressure transducer), sensor backhaul, and a rechargeable 20 Ah battery. As with its dry-barrel counterpart, the wet-barrel configuration was designed such that the retrofitted hydrant remained fully functional.



Figure ES-1. Hydrant.AI for Wet Barrel Hydrants.

### 3.1 TEST DESIGN

Selection of the demonstration site and hydrants for installation of the sensor stations was accomplished through extensive consultation with NAVFAC EXWC and NBVC staff. The northwest corner of NBVC, Port Hueneme was selected as the demonstration site with consideration to various factors such as ease of access and minimal disruption to routine operations. The demonstration site, location of the sensor stations and presumed layout of the underground pipe network is shown in Figure ES-2. An example of a wet barrel hydrant, as retrofitted with the hydrant.AI sensor station, is shown in Figure ES-3.



Figure ES-2. Demonstration Site Map.



Figure ES-3. Wet Barrel Hydrant, as Retrofitted with hydrant.AI Sensor Station at NBVC Port Hueneme Demonstration Site.

The technology was demonstrated in two phases. Phase-I demonstrated an offline, asynchronous deployment of the technology where the standard cellular communications module in the device was replaced with a local storage module. Data from the devices was manually collected and transferred to the server at scheduled intervals. In Phase-II, the wireless communication daughter card was re-installed, enabling cellular communication with the standalone server and global positioning system (GPS) connectivity which allowed for real-time delivery of sensor data and over-the-air updating of sampling/collection parameters (Figure ES-7). Figure ES-4 shows the high-level system architecture of the technology as deployed in Phase-II. This phased approach also allowed the demonstration to commence while securing necessary cybersecurity approvals for wireless data transfer. Separate approvals, granted through limited test event applications, were required for each phase and authorized operation for six months.

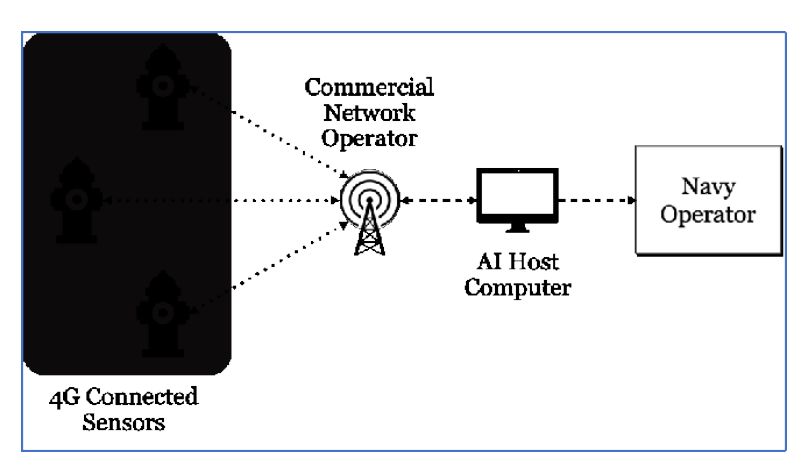


Figure ES-4. High-level System Architecture (Phase-II).

### 3.2 DEMONSTRATION TESTS

To ensure that the technology could be evaluated in the absence of naturally occurring leaks in the WDN, leaks were simulated through controlled flow testing (5-30 gallons per minute (GPM)) at several locations, comprised of two hydrants in the demonstration area and a sampling station located near hydrant 2 (shown in Figure ES-5). Preliminary flow tests in Phase-I used leaks simulated through the manual operation of the valve or hydrant nozzle, where the flow rate was verified by measuring the time required to fill a container of known volume. Details of the preliminary testing are shown in Table ES-1.

Following preliminary validation, subsequent tests were performed using an automatic leak simulator as shown in Figure ES-6, which provided the flexibility to simulate leaks at any time of the day. This method was considered practically advantageous as the tests could be scheduled to automatically trigger the opening of the valve at a precise flow rate and time of day. The automatic leak simulator was set to trigger overnight for a short duration during the period of minimum background noise. To emulate a longstanding leak in the WDN, the automated leak simulations in Phase-I ran from Feb to May 2023, the details of which are listed in Table ES-2. In Phase-I, a total of 79 flow tests were conducted. One test was performed every 24 hours and consisted of the following cycle of events in the order: (i) no-leak – (ii) leak – (iii) no-leak. The acquired data from daily automatic leak simulation was manually retrieved by connecting a laptop to the hydrant retrofits on a bi-weekly basis. The data acquired on the laptop was then transferred to the standalone server in UCLA where the data processing and analysis was conducted. A similar test plan was adopted in Phase-II, with details shown in Table ES-3. With the availability of cellular connectivity, data from the Phase-II testing was transmitted to the server in real-time.

The acoustic data collected from both Phase-I and II was subsequently used to train and validate the leak detection and localization algorithms. The limited amount of data available in Phase-I was conducive to the deployment of unsupervised anomaly detection-based machine learning models for leak detection. Relative to other types of machine learning models, anomaly detection models can be deployed with significantly less training data and requires only data from one case (i.e., non-leak case). In Phase-II, with sufficient labelled data available, a more powerful set of supervised machine learning models was deployed for leak detection, replacing the anomaly detection models used in Phase-I.



Figure ES-5. A Leak Simulated at the Sampling Station During Phase-I Testing.



Figure ES-6. An Apparatus Attached to a Hydrant for Automating the Leak Flow.



Figure ES-7. hydrant.AI Sensor Backhaul with a Wireless Communication Module for Phase-II.

Table ES-1. Details of a Flow Test Conducted at the Location: Sampling Station | Phase-I | 19 Jan 2023.

Condition	Duration (minutes)	Location	Start time	Finish time
Baseline – No leak	20	-	11:00 AM	11:20 AM
Light leak (8.5 GPM)	10	Sampling Station	11:20 AM	11:30 AM
Baseline – No leak	20	-	11:30 AM	11:50 AM
Hard leak (25.5 GPM)	10	Sampling Station	11:50 AM	12:00 PM
Baseline – No leak	20	-	12:00 PM	12:20 PM

Table ES-2. Details of Automated Flow Tests Conducted Overnight Over Multiple Days | Phase-I.

Range of dates for overnight flow tests	Location	Flow rate (GPM)		
16 Feb 2023 – 17 Feb 2023	Hydrant 2	30		
18 Feb 2023 – 23 Feb 2023	Hydrant 2	10		
24 Feb 2023 – 20 Apr 2023	Hydrant 2	20		
21 Apr 2023 – 4 May 2023	Fire Suppression System	10		

Table ES-3. Details of an Automated Flow Test Conducted at the Location Hydrant 2 | Phase-II | 1 Nov 2023–1 Mar 2024.

Condition	Duration (minutes)	Location	Start time	Finish time
Baseline – No leak	5	ı	12:50 AM	12:55 AM
Hard leak (30 GPM)	15	Hydrant 2	12:55 AM	01:10 AM
Baseline – No leak	13	-	01:10 AM	01:23 AM

### 4.0 PERFORMANCE ASSESSMENT

A summary of all data analysis conducted in support of the assessment of the performance objectives is presented hereafter.

### 4.1 BASELINE LEARNING

The AI leak detection models were built upon a foundation of both labelled and unlabeled acoustic baseline data collected over various time periods spanning from December 2022 to January 2023. During these data collection phases, particular emphasis was placed on gathering information during the late-night hours between 2-5 AM, a period characterized by minimal usage activity within the distribution network. Acoustic data was pre-processed to remove outliers and transformed into leak-sensitive features for training the leak detection models. The importance of using leak-sensitive features as inputs to the leak detection models as opposed to raw acoustic data can be shown using the acoustic data collected from the 19 Jan 2023 daytime flow test in Figure ES-8. Due to the high background noise present during the day, the simulated leaks in Figure ES-8 showed no discernable change in the raw acoustic noise. Hence, a machine learning model trained on the raw acoustic noise would not be able to detect the simulated leaks. The leak-sensitive features used in Phase-I were developed specifically by DWS for such scenarios—to detect leaks obscured by background noise. An example of how the leak-sensitive features were able to separate leak data from non-leak data is shown in Figure ES-9. An overview of the main steps involved in baseline learning and leak detection model training and testing are shown in Figure ES-10.

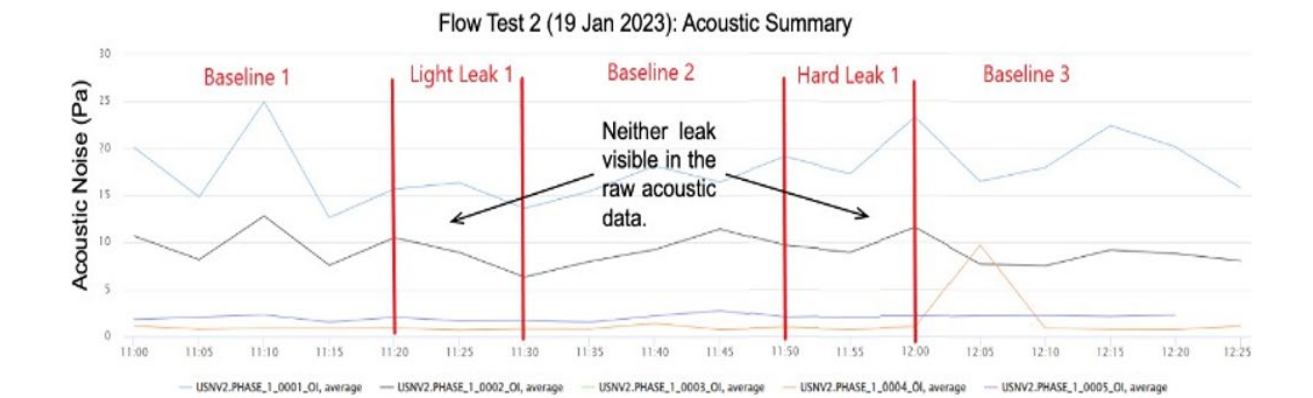


Figure ES-8. Acoustic Summary for Flow Test with Details Shown in Table ES-1.

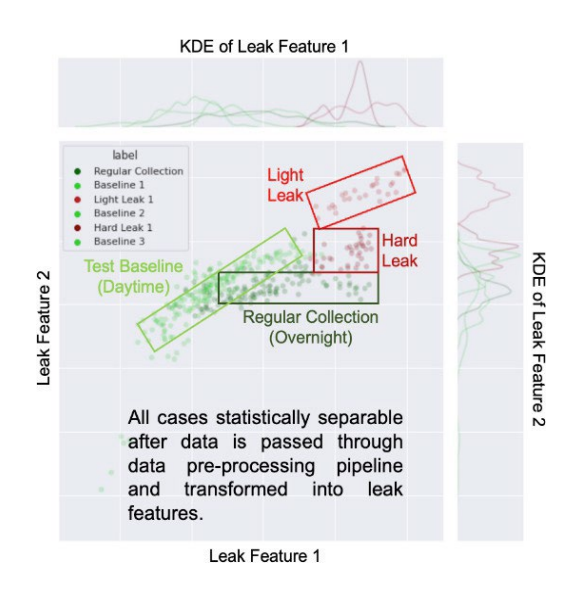


Figure ES-9. Scatterplot and Corresponding Kernel Density Estimates of Acoustic Data from a Flow Test (ref. Table ES-1), after Transformation of Data into Leak Features.



Figure ES-10. Overview of Baseline Learning & Leak Detection Model Testing Procedure.

### 4.2 LEAK DETECTION

Features extracted from the acoustic data were used to train a suite of 11 unique, machine-learning models. For Phase-I, the minimum accuracy returned by the best AI leak detection model for each hydrant, across three different simulated leak events is shown in Table ES-4. Table ES-4 also shows that the performance of the AI leak detection models was consistent across hydrants and flow tests. The error margin across all three flow tests can be attributed to several factors, including erroneous or mislabeled points in the dataset and the limitation on the type of viable machine models given the limited amount of data available in Phase-I.

Insights from time-frequency analysis led to improvements in Phase-II's leak detection process. These included modifications to the filter bank used for pre-processing, enhancing the distinction between nearby and distant leaks. The F1 scores (a measure of a model's accuracy) for each model from the baseline and leak detection in Phase-II are shown in Figure ES-11a and ES-11b, respectively. During baseline learning (Figure ES-11a), the XGBoost and GBM Classifier models were identified as the best-performing models, achieving the maximum F1 score of 100% across all hydrants. During the leak detection phase (Figure ES-11b), the XGBoost model continued to achieve the highest overall F1 score, with a minimum F1 score of 98% observed on Hydrants 3 and 4. Similarly, strong performance between the baseline and leak detection phases verified that the models were not overfitting the training data, with only a marginal reduction in F1 score of 1-3% observed on Hydrants 1, 3 and 4.

Table ES-4. Minimum Accuracy Returned by AI leak detection models on test datasets.

Evaluation Metric	Test Case	Flow	Flow Hydrant					Overall
Evaluation Metric	Test Case	Rates	1	2	3	4	5	Overall
AI Leak Detection Minimum AI Leak Detection Model Accuracy	Flow Test 1 - Daytime (Peak System Usage)	5-10 gal/min flow	93.80%	96.70%	98.00%	99.50%	97.60%	97.1%
	Flow Test 2 - Daytime (Peak System Usage)	8-25 gal/min flow	95.70%	94.90%	100%	97.70%	96.20%	96.9%
	Flow Test 3 - Nighttime (Low System Usage)	10 ,20, 30 gal/min flow		100.00%			93.50%	96.8%

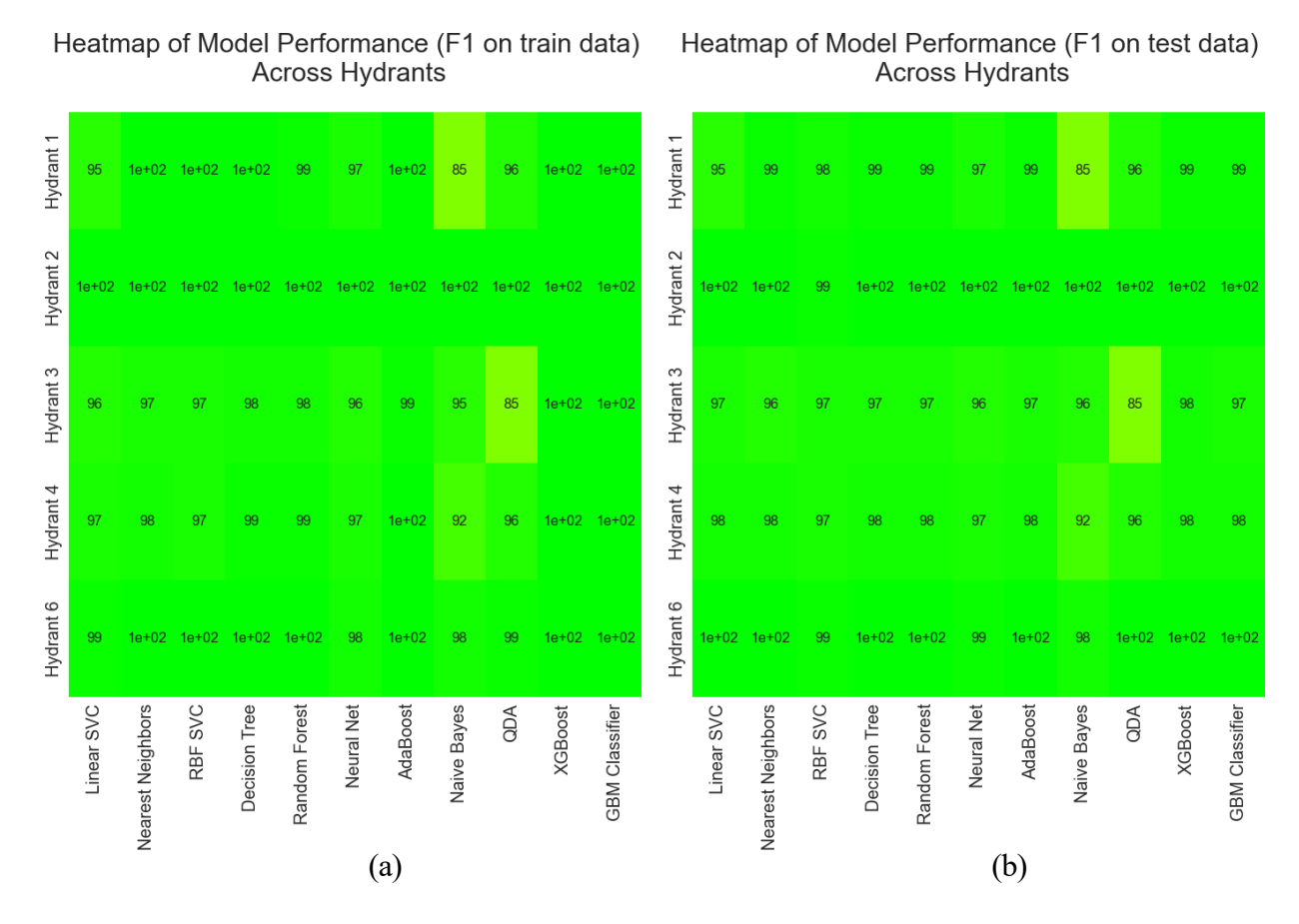


Figure ES-11. Heatmap of Model Performance Across Hydrants for: (a) Baseline (b) Leak Detection.

### 4.3 TRANSIENT PRESSURE DETECTION

The transition to wireless communications in Phase-II provided the ability to detect, capture, and relay potential structural damaging pressure transients and pressure pattern anomalies in the network in real time. Transients were automatically captured by the device when the pressure measured on the device exceeded a set of user-defined thresholds. When a transient capture was triggered, a complete waveform of the transient event was generated by saving the raw data sampled from 30 seconds preceding the event trigger to 120 seconds following the trigger. These sampling parameters are also user-configurable. An example of a pressure transient captured by the hydrant. AI system is depicted in Figure ES-12. Each transient event detected in the system would generate an "Event Card" on the user interface, which could be accessed to view the detailed waveform as shown in Figure ES-12. In addition, an email or SMS alert could be configured to notify the appropriate parties immediately to enable a timely response, if necessary.



Figure ES-12. Snapshot of a Pressure Transient Captured by the hydrant.AI System at Hydrant 3.

### 4.4 LEAK LOCALIZATION

The leak locations were estimated using a probabilistic method developed at UCLA [3]. The method used cross-correlation-based maximum likelihood estimation (MLE) to estimate the most likely location between two sensor pairs using the filtered acoustic measurements at the sensor locations. In the step involving time delay selection from cross-correlation function plots, a threshold was set to estimate the leak location. It was found that this threshold affected the leak location. The leak location estimate for an optimal threshold is shown in Figure ES-13 for Phase-I and Phase-II testing (details of the tests were mentioned in Tables ES-1 and ES-3). In Phase-I, the simulated leak was at the sampling station; however, for Phase-II the simulated leak was shifted to Hydrant 2 due to its compatibility with the automated leak equipment.

The distance between the leak estimate and the actual leak location were 21 m and 32 m for Phase-I and Phase-II results, respectively. The errors were primarily attributed to the following: (a) inaccurate pipeline topographical maps leading to large uncertainties in the estimated pipe lengths; and (b) the clock drift in the crystal-based real-time clocks used in the sensor stations leading to desynchronization in measured time thereby yielding errors in the time delays of arrival. The localization results were promising, considering that, even with these large uncertainties, the localization results were localized to the pipe segment level (hence, satisfying the performance criteria) and were within 5% of the total pipeline length in the WDN in which the leak search was performed. It is important to underscore that the localization aspect of this technology was only meant to provide an approximate region where the leak was present. Once a leak was detected and localized to a region, the expectation was that inspection and maintenance crews would be deployed to pinpoint the leak for repair activities.

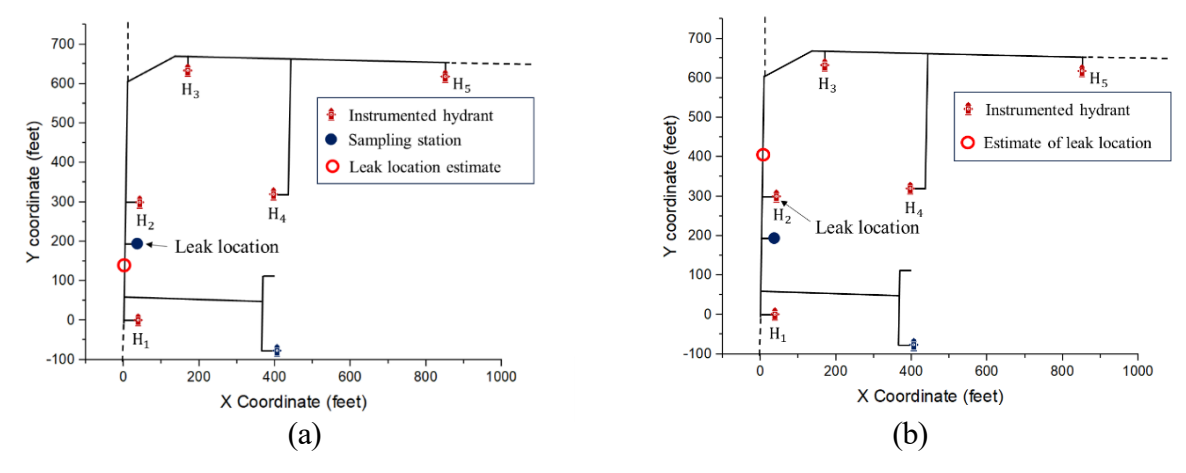


Figure ES-13. Leak Location Estimate Obtained for an Optimal Cross-correlation Threshold from a Leak Simulated at (a) the Sampling Station for Data Acquired at 11:54 AM on 19-Jan-2023 (Phase-I), (b) Hydrant 2 for Data Acquired as 12:52 AM on 3-Nov-2023 (Phase-II).

### 5.0 COST ASSESSMENT

A simple cost analysis for the technology was constructed by evaluating primary costs against expected returns for a 5-unit deployment in a known high-risk or trouble region where leaks and water loss are expected to be found. The analysis was conducted over the 10-year expected useful life of the sensing stations. The main cost factors for this model comprised non-recurring capital costs (e.g., sensing stations, batteries) and installation costs and annually recurring operating costs (e.g., server upkeep, cellular data plans). The total capital cost for a 5-unit deployment (1 additional spare unit and battery) in year 1 was determined to be \$66,750, and the annual operating cost was determined to be \$5,700.

The implementation of these sensors allowed for the identification and repair of existing leaks as well as subsequent early detection and prevention of new leaks within the monitored area of the network. Consequently, the expected water savings or return on investment (ROI) could be assumed to be constant year-over-year. The assumptions result in a linear relationship between the number of the units deployed and cost or ROI, allowing the calculation to be scaled to any size of deployments or capital investment.

Two types of leaks were considered in the water savings calculations: small, non-surfacing leaks (5-30 GPM) which can run undetected for upwards of a year at a time; and, larger, sudden leaks or breaks, which typically exhibit significantly higher flowrates (100-122 GPM), but surface shortly after forming. The average annual 2024 water rate of \$10.27/kgal for NBVC Port Hueneme was used as the cost basis for the analysis. Based on these parameters, the estimated range for the total expected annual water savings of the system was determined to be between \$38,400 and \$177,000.

The life cycle cost analysis using the average of these two extremes, is shown in Table ES-5, and demonstrates that the payback period where the water savings exceeds the net present value occurs within the first year, showing that the system can quickly recoup the initial capital investment immediately through identification and subsequent repair of existing but unknown leaks in the distribution system.

Table ES-5. Life-cycle Cost Analysis.

Life-cycle Cost Analysis - 5 Sensors						
Year	Discount Factor	Operating Costs	Expected Water Savings	Net Present Value		
0	1.0000	\$ (5,700)	\$ 107,784	\$ 40,409.5		
1	0.9709	\$ (5,534)	\$ 104,645	\$ 139,520.6		
2	0.9426	\$ (5,373)	\$ 101,597	\$ 235,745.0		
3	0.9151	\$ (5,216)	\$ 98,638	\$ 329,166.8		
4	0.8885	\$ (5,064)	\$ 95,765	\$ 419,867.5		
5	0.8626	\$ (4,917)	\$ 92,976	\$ 507,926.5		
6	0.8375	\$ (4,774)	\$ 90,268	\$ 593,420.6		
7	0.8131	\$ (4,635)	\$ 87,639	\$ 676,424.6		
8	0.7894	\$ (4,500)	\$ 85,086	\$ 757,011.0		
9	0.7664	\$ (4,369)	\$ 82,608	\$ 835,250.3		
10	0.7441	\$ (4,241)	\$ 80,202	\$ 911,210.7		

### 6.0 IMPLEMENTATION ISSUES

The implementation issues encountered throughout the project can be categorized into regulatory/cybersecurity-related or technical-related. Several measures were taken to mitigate the regulatory or cybersecurity-related barriers to implementation. The development and testing of an 'offline' version of the monitoring technology in Phase-I was one such approach. While viable, the drawbacks of an offline deployment, such as the asynchronous nature of data collection and information delivery, motivated the pursuit of the wireless implementation in Phase-II. In Phase-II, it was determined that DoD deployment of the wirelessly interconnected AI leak detection system would require an Authority to Operate (ATO) to maintain imposed cybersecurity protocols per DoD Instruction 8510.01, Risk Management Framework (RMF) for DoD Information Technology. In an effort to expedite the ATO process for future deployments, a partial, site-agnostic RMF package was developed for the system in Phase-II. The RMF package was expected to reduce documentation development efforts by between 70 to 80 percent and subsequently the time necessary to obtain a final ATO.

In Phase-I, the primary technical issues encountered during the demonstration were all in relation to the lack of wireless connectivity between the sensing stations, GPS satellites, and central server. The lack of wireless connectivity meant that data collection was asynchronous, requiring an individual to physically travel to each sensing station to collect data from each device for transfer to the central server. The asynchronous nature of the data collection meant that potential actionable information pertaining to leaks or pressure events could not be delivered in real-time. Additionally, precise time synchronization between devices for leak localization between devices was also difficult to achieve. The addition of wireless communication and GPS modules in Phase-II helped to alleviate most of the concerns identified in Phase-I, enabling data and model insights to be delivered in real-time. Furthermore, the GPS was able to act as a datum for clock synchronization.

While the addition of GPS resulted in a noticeable improvement in localization accuracy, additional precision in clock synchronization (in addition to good quality data on the pipe configurations) would be required to further reduce localization errors. Further changes to improve the time synchronization across devices were identified at the end of Phase-II and will be implemented in the firmware for future deployments.

### 7.0 REFERENCES

- [1] S. Folkman, "Water Main Break Rates In the USA and Canada: A Comprehensive Study," 2018, [Online]. Available: https://digitalcommons.usu.edu/cgi/viewcontent.cgi?article=1173&=&context=mae\_facpub &=&seiredir=1&referer=https%253A%252F%252Fscholar.google.com%252Fscholar%253 Fhl%253Den%2526assdt%253D0%25252C5%2526q%253DFolkman%252BUtah%252Bwa ter%2526btnG%253D#search=%22Folkman%20Utah%20water%22.
- [2] G. M. Baird and S. Folkman, "Recent Survey Results of Water Main Failures in the U.S. and Canada." Pipelines 2019, Jul. 18, 2019. [Online]. Available: https://doi.org/10.1061/9780784482506.001
- [3] M. D. Kafle, S. Fong, and S. Narasimhan, "Active acoustic leak detection and localization in a plastic pipe using time delay estimation," *Appl. Acoust.*, vol. 187, p. 108482, Feb. 2022, doi: 10.1016/j.apacoust.2021.108482.